Hindawi Publishing Corporation
Journal of Chemistry
Volume 2013, Article ID 234904, 13 pages
http://dx.doi.org/10.1155/2013/234904

Research Article

Full Factorial Experimental Design Analysis of Reactive Dye Removal by Carbon Adsorption

N. Özbay, A. Ş. Yargıç, R. Z. Yarbay-Şahin, and E. Önal

Chemical and Process Engineering Department, Engineering Faculty, Gulumbe Campus, Bilecik Seyh Edebali University, 11210 Bilecik, Turkey

Correspondence should be addressed to A. Ş. Yargıç; seyda.guler@bilecik.edu.tr

Received 28 May 2013; Revised 22 July 2013; Accepted 24 July 2013

Academic Editor: Subrata Mondal

The objective of this study was to investigate the removal of Remazol Yellow dye from aqueous solutions by adsorption on activated carbon prepared by chemical activation of sunflower seed cake. It was found that the carbon content of biomass increases up to 65.12% after activation and carbonization processes. The maximum percentage dye removal was obtained as 82.12% with 0.4 g/50 mL adsorbent dosage at 313 K. The Langmuir model showed the best fit with equilibrium isotherm data. The interactions were evaluated with respect to both pseudo-first-order and pseudo-second-order reaction kinetics. The adsorption process was found to follow the pseudo-second-order model. To optimize the operating conditions, the effects of pH, adsorbent dosage, and initial dye concentration were investigated by full factorial experimental design method; adsorbent dosage was found as the most significant factor with $P = 0.02$ lower than 95% confidence level. The obtained results are very promising since (i) the utilization of sunflower seed cake activated carbon (SSCAC) played a critical role in the adsorption of dye; (ii) sunflower seed cake was an intriguing, low-cost, and easily available material. It can be an alternative adsorbent precursor for more expensive adsorbents used for Remazol Yellow (RY) removal.

1. Introduction

Rapidly changing technologies, industrial products, and applications are causing worldwide waste problem and contaminating the environment. If waste products are improperly managed, public health and the environment could be threatened [1, 2]. Among all industrial sectors, textile industries are rated as high polluters, taking into consideration the volume of discharge and effluent composition [1, 3]. Globally, thousands of the dye stuffs are being synthesized daily and also being released in the environment in the form of effluents during synthesis and dyeing processes [4]. Most of the dyes decompose to give out hazardous products, such as carbon monoxide (CO), carbon dioxide (CO_2), nitrogen oxides, and hydrogen chlorides, and can reduce light penetration and photosynthesis [5].

Currently, synthetic dyes are largely used in many fields, for example, in various branches of the textile industry, in leather tanning industry, in paper production, in food technology, in agricultural research, in light-harvesting arrays, in photoelectrochemical cells, and in hair colorings [6–15]. The wastewater from textile and dyestuff industries is characterized by high alkalinity, biological oxidation demand, chemical oxidation demand, and total dissolved solids with dye concentrations generally below 1 g/dm^3 [16, 17]. Reactive dyes are the most common dyes used due to their favorable characteristics of bright color, water fastness, simple application techniques, and low energy consumption. They exhibit a wide range of different chemical structures, primarily based on substituted aromatic and heterocyclic groups [18, 19]. They are not easily biodegradable; thus, the color may remain in the effluent even after extensive treatment [18, 20].

Dye wastewater is usually treated by physical or chemical treatment processes. These include flocculation combined with flotation, electroflocculation, membrane filtration, electrokinetic coagulation, electrochemical destruction, ion-exchange, irradiation, adsorption, precipitation, ozonation, and katox treatment methods involving the use of activated carbon and air mixtures. However, these technologies are generally unsuccessful in color removal, expensive, and less

adaptable to a wide range of dye wastewaters [16, 21]. The low cost, simple design, easy handling, and sludge-free cleaning operations have established the adsorption technique as more effective and convenient in comparison to other techniques [1, 22].

Adsorption now plays a key role in modern industries, mainly in the field of environmental protection engineering, with the increasing environmental consciousness of people all over the world. Adsorption processes are being employed widely for large-scale biochemical, chemical, and environmental recovery and purification applications [23]. Over the last few decades, adsorption has been recognized as an influential separation process and has become an attractive option for the removal of dyes from industrial effluents [24]. Adsorbents are used in various processes; activated carbons are among the most effective adsorbents because of their excellent adsorption capacity for organic targets [24]. Many studies have been undertaken to investigate the use of low-cost adsorbents such as peat, bentonite, steel-plant slag, fly ash, china clay, maize cob, wood shavings, silica [16, 25–27], bacterial biomass and biopolymers [22, 28], coir pith [20], sugar beet pulp [29], sugarcane bagasse pith [30], jute fiber [19, 31], hen feathers [32], soybean [33, 34], and wheat husk [35] for color removal. Unfortunately, these low-cost adsorbents have generally low adsorption capacities and require large amounts of adsorbents. Therefore, a need arises to find new, economical, easily available, and highly effective adsorbents [16].

Sunflower *(Helianthus annuus L.)* is one of the foremost oil seed crops cultivated for the production of cooking oil [36]. The total world production of 38 million tons of sunflower seed, grown on about 25 million hectares [37], go almost exclusively to oil extraction, providing 8.2% of total world volume, estimated at around 107 million tones [38, 39]. In Turkey, sunflower is grown in the Thrace, the Aegean, and the Black Sea regions for oil production; thus, Turkey is one of the major sunflower producers and exporter countries. Oil extraction from the seeds is accompanied by the coproduction of lignocellulosic biomass, in the form of sunflower seed hulls, which comprise 30% of the sunflower seeds. These residues are usually disposed of by burning or by deposition in landfills, but conversion to higher-value products would be preferable. One such product could be activated carbon [36].

No information is available on Remazol Yellow removal from aqueous solution by sunflower biomass in the literature. This low-cost material may be especially suitable for various applications in developing countries and small-scale industries. Consequently, the scope of this study was not only to produce chemically activated sunflower seeds as an alternative low-cost adsorbent for removal of Remazol Yellow dye from aqueous solutions, but also to characterize it and to investigate the effects of operating parameters such as solution pH, adsorbent dosage, initial dye concentration, temperature, contact time, and electrolytes used. Equilibrium isotherm data were fitted to Langmuir and Freundlich equations and constants of isotherm equations were determined. Furthermore, pseudo-first and second-order kinetic models were also used to analyze adsorption kinetics. Finally, the most effective parameter (pH, adsorbent dosage, and initial dye concentration) in the adsorption process for dye removal was defined by using Full Factorial Design method and analysis of variance (ANOVA) statistical approach.

2. Materials and Methods

2.1. Preparation of Sunflower Seed Cake Adsorbent and Aqueous Dye Solutions. Sunflower seed cake (SSC) obtained from Central Anatolia region of Turkey was air dried, crushed, and sieved to obtain mean sizes. Bulk density of chosen size was calculated about 0.47 g/cm^3. Sunflower seed cake with reduced particle size was modified by impregnation with 50% wt NH_4Cl solution and dried at 100°C in an oven. Chemical treatment with NH_4Cl was applied to help break down the lignin complex in order to improve the performance of the adsorbent. Modified biomass material was then carbonized at 350°C to produce activated carbon (green carbon) at low temperature, washed with distilled water until the pH of the washing solution reached 6-7, and dried at ambient temperature. Finally, sieved biomass and dried sunflower seed cake activated carbon (SSCAC) were stored in plastic bottles for further use.

Reactive textile dye Remazol Yellow (RY) was used without purification. Dye solutions were prepared using distilled water to prevent and minimize possible interferences. Stock solution of dye was prepared by dissolving 1.0 g of RY dye in 1000 mL of distilled water. By diluting the standard solution of dye, different working concentrations (50–250 mg/L) were arranged.

2.2. Methodologies Used for Low Temperature Activated Carbon Characterization. Different characterization techniques have been used to identify the produced activated carbon and the main constituents of the sunflower seed cake activated carbon. This will now be discussed. The ultimate analysis of SSC and SSCAC was performed using Elemental Analyzer (Leco CNH628 S628) to find carbon, hydrogen, nitrogen, and oxygen contents of materials by using helium, dry air, and oxygen gases. The complete combustion of all organic samples was carried out by operating Elemental Analyzer's furnace at 950°C. Structure and preliminary analyses were carried out to complete the proximate analysis of SSC. Functional groups of SSC and SSCAC were estimated by Fourier transform infrared (FTIR) spectroscopy (Perkin Elmer Spectrum 100). The FT-IR spectrums of SSC and SSCAC were obtained using the ATR technique (with a diamond protected Attenuated Total Reflectance crystal unit) with a resolution of 4 cm^{-1} after 100 scans. Surface morphologies of SSC and SSCAC were observed by employing a scanning electron microscope (Zeiss Supra VP 40) with an accelerating voltage of 5 kV. The samples were sputter-coated with platinum (Quorum Q 150 R ES DC Sputter).

2.3. Batch Adsorption Studies. The effects of important parameters such as pH, adsorbent dosage, initial dye concentration, temperature, contact time, and electrolyte on the adsorption of Remazol Yellow were studied. Batch adsorption experiments were conducted in a set of conical flasks containing 50 mL dye solution of different operating conditions until the equilibrium was reached. The suspensions were then

filtered and dye concentrations in the supernatant solutions were measured. Standard curves were developed at λ_{max}, 422 nm for Remazol Yellow dye, through the measurement of the dye solution absorbance by UV/Visible Spectrophotometer (V-530 Jasco UV/VIS).

The amount of dye adsorbed per unit mass was calculated using the following equation [18]:

$$q_e = \frac{(C_0 - C_e)V}{W}, \quad (1)$$

where q_e is the amount of dye adsorbed on the adsorbent (mg/g), C_0 and C_e (mg/L) are the liquid phase concentrations of dye at initial and equilibrium, respectively. V (L) is the volume of dye solution and W (g) is the amount of the green carbon used. The dye removal efficiency was defined as [18]

$$\eta = \left(\frac{C_0 - C_e}{C_0}\right)100. \quad (2)$$

2.4. Kinetic and Isotherm Models. Interaction of adsorbate with the adsorbent materials is indicated by the adsorption isotherm. It is important to establish the most appropriate correlations for the equilibrium data of the system for optimizing the design of adsorption process to remove RY dye. The experimental data of RY dye was analyzed using linear Langmuir and Freundlich isotherm models to investigate the effect of temperature on the equilibrium capacity of SSCAC. Linear regression is generally used to find which isotherm is best fitted, and also the correlation coefficients of R^2 are evaluated to compare the practicality of isotherm equation.

The Langmuir isotherm assumes monolayer adsorption onto a surface containing a finite number of identical adsorption sites [40]. Langmuir theory is based on two assumptions that the adsorbed layer is unimolecular and the forces of interaction between sorbed molecules are negligible [36]. Adsorption is assumed to take place at specific homogeneous sites with the adsorbent. Once a dye molecule occupies a site, no further adsorption can take place at that site. The linear form of Langmuir isotherm equation is represented as [6]

$$\frac{C_e}{q_e} = \frac{1}{K_L q_m} + \frac{C_e}{q_m}, \quad (3)$$

where q_m (mg/g) and K_L (L/mg) are Langmuir constants related to maximum adsorption capacity and rate of adsorption, respectively. Also, q_e (mg/g) is the amount of dye adsorbed per unit weight of adsorbent, C_e (mg/L) is the concentration of the dye solution at equilibrium. q_m and K_L values are obtained from the slope and intercept of the linear plot (C_e/q_e is plotted against C_e).

The Freundlich isotherm assumes heterogeneous surface energies on the adsorbent surface [41], in which the energy term in Langmuir equation varies as a function of the surface coverage. A linear form of the Freundlich equation is derived by [42]

$$\log q_e = \log K_F + \frac{1}{n}\log C_e, \quad (4)$$

where K_F (mg/g(L/mg)$^{1/n}$) and n are the Freundlich adsorption constant and heterogeneity factor, respectively. K_F is related to the bonding energy and $1/n$ value is related to the adsorption intensity. The intercept K_F and the slope $1/n$ are obtained by plotting ln q_e versus ln C_e.

To illuminate the possible mechanism of RY dye adsorption process, pseudo-first-order and pseudo-second-order kinetic models were tested by using the data obtained from adsorption kinetic experiments.

The pseudo-first-order kinetic model of Lagergren is extensively studied and defined as [43]

$$\log(q_e - q_t) = \log q_e - \frac{k_1 t}{2.303}, \quad (5)$$

where k_1 is the rate constant of pseudo-first-order adsorption (min^{-1}), t is the contact time (min), and q_e and q_t (mg/g) are the amounts of RY adsorbed at equilibrium and at time t (min), respectively [18]. By using this linear equation and drawing a plot of $\log(q_e - q_t)$ versus t, the slope of $(-k_1/2.303)$ and the intercept of $(\log q_e)$ are obtained.

The pseudo-second-order model estimates the behavior over the whole range adsorption [18] and this model is also based on the adsorption capacity of the solid phase. The pseudo-second-order model has a supposition that the sorption process involves chemisorption mechanism and is defined as [38]

$$\frac{t}{q_t} = \frac{1}{k_2 q_e^2} + \frac{1}{q_e}t, \quad (6)$$

where k_2 is the rate constant of pseudo-second-order adsorption (g/mg · min), t is the contact time (min), and q_e and q_t (mg/g) are the amounts of RY adsorbed at equilibrium and at time t (min), respectively [38]. If pseudo-second-order kinetic equation is suitable, q_e and k_2 can be determined experimentally from the slope and intercept of plot t/q_t versus t [44].

2.5. Full Factorial Design of Experiments. Previously planned experimental design, which examines all factors at once, has been used widely instead of conventional experimental design, which investigates every variable by changing one by one. Optimum conditions are decided by changing several factors at once and using different levels of these factors. Factorial designs are widely applied in the experiments that are taking into account several factors where it is necessary to study the interaction effect of factors on the response [45]. 2^n factorial design of experiments needs less number of experiments for several factors; thus, materials and time used are slightly reduced [46, 47]. When factorial design methods applied to experiments of a process, mathematical models are derived through obtained variance analysis tables. If the model is seen insufficient, it can be varied and new experiments are prepared until the most appropriate model is achieved. Experiments are chosen randomly to prevent partiality of researchers.

The factorial design describes which factor shows more impact and influences the variation of one factor on the other factors [48]. The three factors pH, adsorbent dosage,

Table 1: High and low levels of factors.

Factors	Low level (−1)	High level (+1)
pH	2	8
Adsorbent dosage (g/L)	2	8
Initial concentration (mg/L)	100	250

and initial concentration of dye were varied at two levels as given in Table 1 to investigate their effects on RY dye removal (%). Experiments for full factorial design were conducted in a set of conical flasks containing 50 mL dye solution of known pH, concentration, and adsorbent dose for 1 h at 293 K until the equilibrium was reached. After one hour of contact time, the suspensions were filtered and dye concentrations in the supernatant solutions were measured using a UV-vis spectrophotometer.

3. Results and Discussion

3.1. Characterization of SSC and SSCAC

3.1.1. Ultimate and Proximate Analysis. The results for ultimate and proximate analyses of sunflower seed cake and ultimate analysis of activated carbon are presented in Table 2. Low ash and high carbon content showed that the sunflower seed cake was suitable for activated carbon production. After undergoing activation process, the carbon content and calorific value increased significantly whereas the oxygen content decreased in the sample, which indicates that activated carbon was more carbonaceous material than sunflower seed cake.

3.1.2. Fourier Transforms Infrared Spectroscopy (FT-IR). The FT-IR spectra can provide valuable information about the chemical compositions of the materials. FT-IR analysis of sunflower seed cake and activated carbon was performed in the range of 4000–380 cm^{-1} in order to explore surface characteristics (see Figure 1). The FT-IR vibrational spectra of the sunflower seed cake and chemically activated low temperature green carbon are shown in Figures 1(a) and 1(b), respectively. The obtained FT-IR spectra revealed that the sunflower seed cake contained more bands than the prepared activated carbon. Note that the surface functional groups of sunflower seed cake experienced chemical changes during NH_4Cl chemical activation and low temperature carbonization processes. Sunflower seed cake consisted of various functional groups on surfaces. The main functional groups were O–H stretching vibration of hydroxyl functional groups including hydrogen bonding which was detected at bandwidths of 3300–3200 cm^{-1} [40], but the weakened O–H vibrations was found at about 3250 cm^{-1} for prepared activated carbon owing to the degradation of lignocellulosic and cellulosic material. Other major peaks detected at 2923 and 2854 cm^{-1} were attributed to symmetric and asymmetric C-H stretching of aliphatic methyl and methylene. Peaks presence at 1743.87 and 1640.68 cm^{-1} represented the carbonyl (–C=O) stretching vibration. Peaks observed at 1535.16 and 1456.27 cm^{-1} were assigned to the aromatic C=C ring stretch. Small band at 1235 cm^{-1} was assigned to CH=CH stretching and also small bands ranging from 1100 to 1000 cm^{-1} were assigned to C–O stretching vibrations of lignin [49]. Peaks located at bandwidths of 700–600 cm^{-1} could be assigned to C–H out-of-plane bending in benzene derivatives. The C–H out-of-plane bending in benzene derivatives was commonly found on the surface of various activated carbons [18].

Table 2: The results for ultimate and proximate analyses.

Ultimate analysis		
Component (%)	Sunflower seed cake	Activated carbon
C	52.15	65.12
N	5.19	9.41
H	7.42	6.63
O[a]	35.26	18.85
HHV (MJ/kg)	28.34	31.04
Proximate analysis of sunflower seed cake		
Preliminary analysis	wt.%	
Moisture	7.72	
Ash	6.17	
Volatile	75.15	
Fixed carbon[a]	10.95	
Structural analysis	wt.%	
Holocellulose	22.90	
Hemicellulose	10.92	
Extractive material	23.59	
Oil	30.30	
Lignin	33.12	
Cellulose[a]	12.53	

[a]Estimated by difference.

3.1.3. Morphological Characterization (SEM). The physical morphologies and surface properties of the sunflower seed cake and activated carbon prepared by chemically activation and low temperature carbonization methods were examined by using scanning electron microscopy (SEM) technique. Figure 2 shows the textural structure investigation of SSC and SSCAC particles from SEM micrograph at 500x and 5000x magnification, respectively. It can be concluded that SEM images of SSC and SSCAC showed severe differences. SSC had a rough surface, and thick wall structure caused a little porosity. Chemical activation and low temperature carbonization methods led opening of thick wall; thus, surface of SSCAC contained more pores than SSC surface and this results in higher surface area.

3.2. Equilibrium Adsorption Edges of Reactive Dye. Various factors that affect the adsorption performance of Remazol Yellow on the activated carbon were examined at equilibrium.

3.2.1. Effect of Solution pH on SSCAC Adsorption. The pH of the dye solution plays an important role in the adsorption capacity, where it affects both the degree of ionization of the dye as well as the surface properties of the adsorbent [6]. In this work, the influence of pH on the dye adsorption was

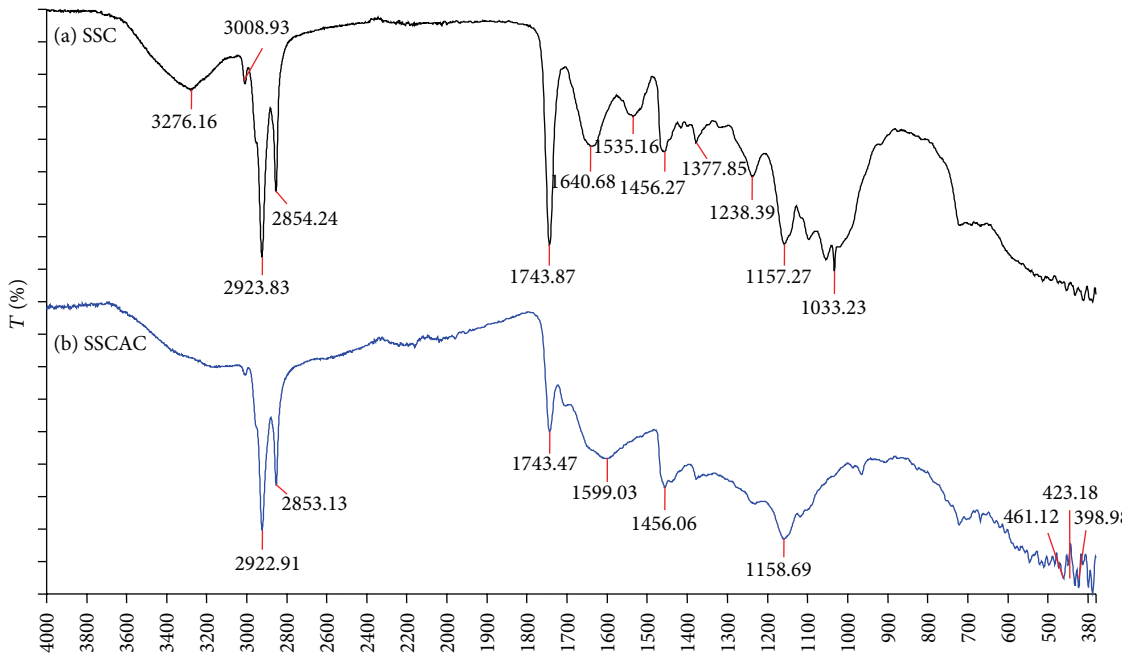

Figure 1: FT-IR spectrums of (a) sunflower seed cake. (b) activated carbon obtained at 350°C.

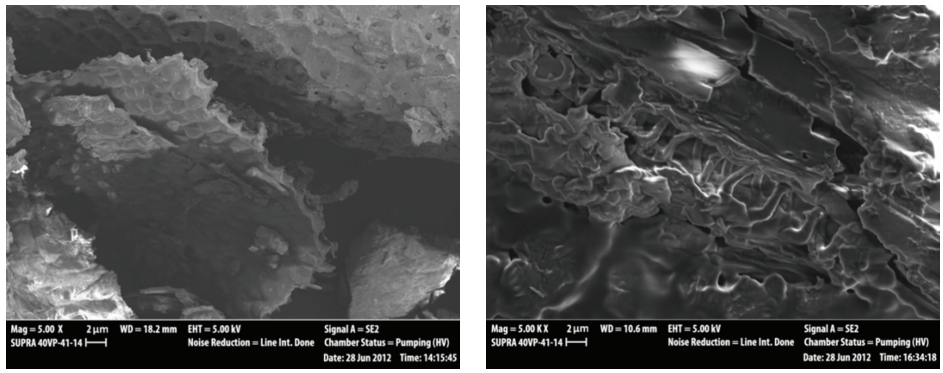

(a) (b)

Figure 2: SEM images of (a) SSC and (b) SSCAC.

studied while the initial dye concentration, contact time, temperature, and amount of SSCAC were fixed at 100 mg/L, 60 min, 293 K, and 0.10 g/50 mL, respectively. The effect of pH on adsorption of dye was studied within pH range 2–8. The pH was adjusted by adding a small amount of 0.1 M HCl and/or 0.1 M NaOH; adjusted pH was measured using pH meter (Thermo Scientific Orion 3 Star). After 60 min equilibration at various pH values illustrated that the percentage adsorption decreased from 22.70% to 7.09% for RY removal when pH increased from 2 to 8 (see Figure 3); thus, the pH value of 2 was selected as the optimum for performing the adsorption studies.

The favorable adsorption of the dye at relatively low pHs in the range of 1.0–5.0 may be attributed to the electrostatic interactions, since at lower solution pH, the SSCAC may get positively charged, which enhances the negatively charged reactive dye anions through electrostatic forces of attraction and hence increase the adsorption capacity [38]. Also, this behavior of dye is in accordance with the known fact that the adsorption decreases with increasing pH for anionic dyes (as the Remazol Yellow in the present case), while it increases with increasing pH for cationic dyes [6].

3.2.2. Effect of Adsorbent Dosage on SSCAC Adsorption. Adsorbent dosage is an important parameter for the adsorption process as it determines the capacity of an adsorbent for a given initial concentration of the adsorbate. The effect of adsorbent dosage for optimum solution pH value of 2 was studied by varying adsorbent amount from 0.1 to 0.5 g/50 mL in increments of 0.05 g. Effects of SSCAC amount on both the percentage dye removal and the adsorption capacity were shown in Figure 4. It was observed that dye removal increased with increasing adsorbent dosage. The percentage dye removals of 61.0% and 69.10% were quite close to each other for 0.4

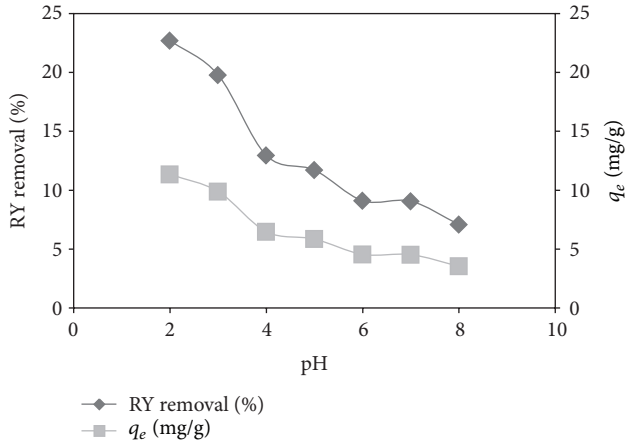

Figure 3: The pH effect for Remazol Yellow adsorption (initial dye concentration: 100 mg/L, contact time: 60 min, temperature: 293 K, amount of SSCAC: 0.1 g activated carbon/50 mL dye solution).

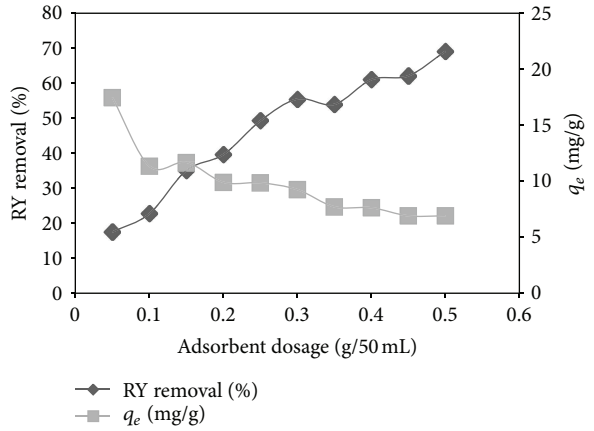

Figure 4: The adsorbent dosage effect for Remazol Yellow adsorption (initial dye concentration: 100 mg/L, contact time: 60 min, temperature: 293 K, pH: 2).

and 0.5 g/50 mL adsorbent dosages, respectively. When low-cost material was considered, 0.4 g SSCAC/50 mL solution was chosen as an optimum dosage. Increase in adsorption with adsorbent dosage can be attributed to increased adsorbent surface area and availability of more adsorption sites [6]. However, the increase in the adsorbent dosage provided a remarkable decrease in the amount of dye uptake per gram of adsorbent (q_e). This could be explained with two factors. First, the increase in adsorbent mass at fixed dye concentration and volume will lead to unsaturation of adsorption sites through the adsorption process, and, second, the reduction in adsorbent capacity is likely to be due to particle aggregation, resulting from high adsorbent mass. Such aggregation would lead to a decrease in total surface area of the adsorbent and an increase in diffusional path length [49]. Hence, the remaining part of the experiments was carried out with adsorbent dosages of 0.1 g/50 mL and 0.4 g/50 mL (w/v) to compare lower and higher adsorbent dosages for RY dye.

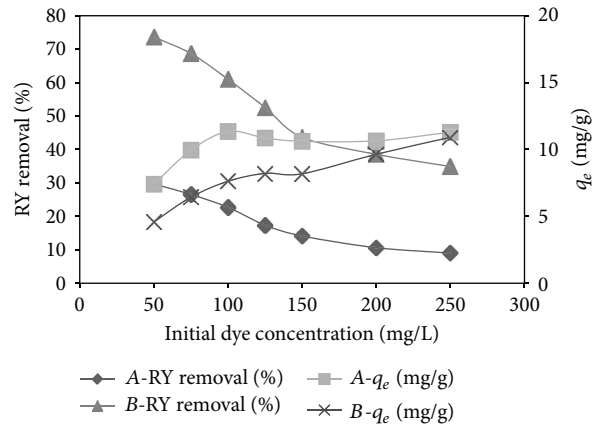

Figure 5: The initial dye concentration effect on adsorption of Remazol Yellow for A = 0.1 g/50 mL and B = 0.4 g/50 mL adsorbent dosages (contact time: 60 min, temperature: 293 K, pH: 2).

3.2.3. Effect of Initial Dye Concentration on SSCAC Adsorption. The effect of initial dye concentration was studied by varying initial dye concentration from 50 to 250 mg/L for 0.4 g/50 mL adsorbent dosage. It has been known that increasing the initial dye concentration results in an increase in the adsorption capacity because the initial dye concentration provides a driving force to overcome mass transfer resistances between the adsorbent and adsorption media [44]. Initially, adsorbate molecules should encounter the boundary layer effect. Then, it should diffuse from boundary layer film onto adsorbent surface and, finally, it should diffuse into the porous structure of the adsorbent [18]. Therefore, at higher initial dye concentration, the number of molecules competing for the available sites on the surface of activated carbon was high, hence, resulting in higher RY adsorption capacities. In the case of lower concentrations, the ratio of dye to the available sorption sites was low and higher adsorption yields were obtained. The adsorption percentage was found to decrease with increase dye concentration. This may be due to the saturation of surface area and active sites of adsorbent [41]. When 0.1 g adsorbent dosage was used, the adsorption uptakes of RY at equilibrium increase from 7.42 to 11.29 mg/g as the initial dye concentration increases from 50 to 250 mg/L. Moreover, when 0.4 g/50 mL adsorbent dosage was used, the adsorption uptakes of RY at equilibrium increase from 4.60 to 10.91 mg/g as the initial dye concentration increases from 50 to 250 mg/L (Figure 5). A similar phenomenon was observed for the adsorption of reactive dyes from aqueous solution on activated carbons [18, 41, 44]. The maximum percentage dye removal of RY was determined as 29.67% at an initial concentration of 50 mg/L for 0.1 g/50 mL adsorbent dosage and 73.61% at an initial concentration of 50 mg/L for 0.4 g/50 mL adsorbent dosage at 293 K. This interesting result shows that high concentration of RY dye attained maximum percentage dye removal even at low adsorbent dosage. Hence, sunflower seed cake activated carbon can be considered an efficient adsorbent for the removal of reactive dye from aqueous solution.

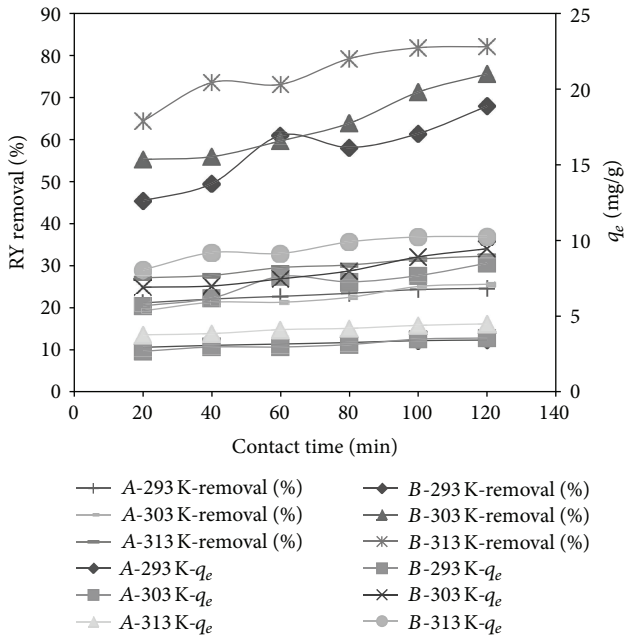

Figure 6: The temperature and contact time effects on dye removal efficiency and adsorption capacity of SSCAC for Remazol Yellow adsorption (adsorbent dosage: A = 0.1 g/50 mL and B = 0.4 g/50 mL, initial dye concentration: 100 mg/L, pH: 2).

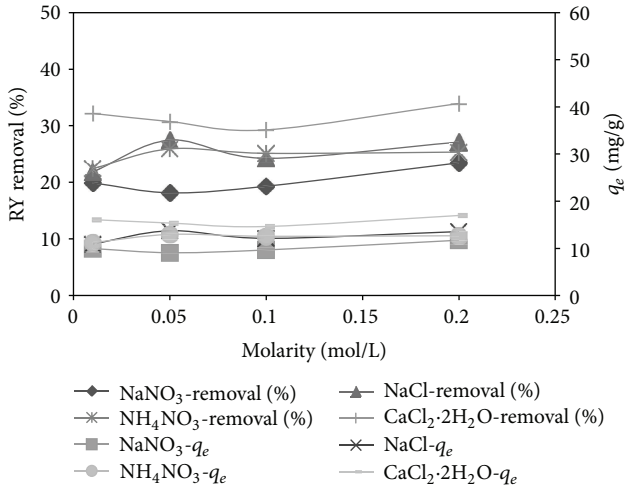

Figure 7: The electrolyte effects on dye removal efficiency and adsorption capacity of SSCAC for Remazol Yellow adsorption (adsorbent dosage: 0.1 g/50 mL, initial dye concentration: 100 mg/L, pH: 2).

3.2.4. Effect of Contact Time and Temperature on SSCAC Adsorption. The adsorption of RY on SSCAC at different temperatures was studied as a function of contact time (20–120 min) in order to determine the equilibrium time; experiments were conducted at 293, 303, and 313 K in an isothermal water bath shaker with initial dye concentration of 100 mg/L and rotation speed of 120 rpm. A rapid adsorption can be seen at the initial stage of the contact period. This is most likely due to a large number of surface sites for adsorption. However, it gradually slowed down until it reached equilibrium. After a lapse of time, the remaining surface sites are difficult to be occupied because of the repulsion between the solute molecules of the solid and bulk phases. Thus, adsorption took long time to reach equilibrium [18]. At the point of dye removal reached a constant value where no more dye was removed from the solution. The amount of dye being adsorbed onto the adsorbent was in a state of dynamic equilibrium with the amount of dye desorbed from the adsorbent. The time required for this state of equilibrium was called the equilibrium time. The amount of dye adsorbed at the equilibrium time reflected the maximum dye adsorption capacity of the adsorbent under these particular conditions [42]. It was indicated that the contact time is needed for RY solution with initial concentration of 100 mg/L to reach equilibrium was 100 min (see Figure 6). The maximum percentage removal of RY was found as 84.12% obtained at 313 K with 0.4 g/50 mL adsorbent dosage. The improvement in adsorption with temperature may be related to an increase in the number of active surface sites available for adsorption on adsorbent, in the porosity, and in the total pore volume of the adsorbent. It could also be due to the decrease in the thickness of the boundary layer surrounding the sorbent with temperature. Therefore, mass transfer resistance of adsorbate in the boundary layer decreases. In addition, this can be a result of an increase in the mobility of the dye molecule with an increase in their kinetic energy and the enhanced rate of intraparticle diffusion of sorbate with the rise of temperature [44]. The results indicated that the adsorption reaction of RY adsorbed by SSCAC was an endothermic process in nature.

3.2.5. Effect of Electrolytes on SSCAC Adsorption. Reactive dyes are the major cause for complaint. Exhaust reactive dyeing required high salt concentration (up to 80 g/L of Na_2SO_4/NaCl); salt is added to shift the equilibrium of dye from the aqueous phase to the solid (fiber) phase [50]. Thus, effects of different electrolytes ($NaNO_3$, NaCl, NH_4NO_3, and $CaCl_2 \cdot 2H_2O$) on the adsorption kinetics were investigated and shown in Figure 7. It was also convenient to study the effect of various salt concentrations (0.01, 0.05, 0.1, and 0.2 M) on the adsorption behavior. Electrolyte effect experiments were carried out with 100 mg/L RY solutions at 293 K and pH of 2. It was found that the addition of these electrolytes to dye solution increased the percentage dye removal and adsorption capacity. The color removal was also dependent on the concentration of added electrolytes. When $CaCl_2 \cdot 2H_2O$ content increased from 0.01 M to 0.2 M, the maximum adsorption capacities for RY increased from 16.09 to 16.97 mg/g. Guelli Ulson de Souza et al. [51] found that the salt addition positively influences the adsorption compared to the experiments achieved without salts. It can be preferred that the salt cations neutralize the negative charge of the carbon surface enabling the adsorption of more molecules or the cations to act directly on the negative adsorbate ions [52].

3.3. Kinetic and Isotherm Models

3.3.1. Equilibrium Adsorption Isotherms. As described previously, the RY adsorption isotherms carried out at 293 K

Table 3: Langmuir and Freundlich coefficients and regression correlation coefficients for adsorption of RY dyes onto SSCAC at 293 K.

Adsorbent dosage (g/50 mL)	Langmuir isotherm			Freundlich isotherm		
	q_m (mg/g)	K_L (L/mg)	R^2	n	K_F	R^2
0.1	11.77	0.0832	0.9920	5.87	4.69	0.5719
0.4	11.91	0.0409	0.9810	3.30	2.31	0.9400

were performed using the optimum experimental conditions. Initial dye concentrations varied as 50, 75, 100, 125, 150, 200, and 250 mg/L, and two different adsorbent dosages 0.1 and 0.4 g/50 mL were used for comparison; all constants and R^2 values obtained by both models are summarized in Table 3. According to Table 3, the highest correlation coefficients (R^2 values) were obtained from Langmuir equation; thus, the Langmuir model displayed better fit to the adsorption data than the Freundlich model. This result indicated that the surface of SSCAC for adsorption of RY was made up of homogeneous adsorption patches.

3.3.2. Adsorption Kinetic Models. Reactive RY dye was adsorbed onto SSCAC with different adsorbent dosages (0.1 and 0.4 g/50 mL) for different time intervals and obtained experimental data were investigated to have a good agreement between pseudo-first-order and pseudo-second-order models. The adsorption rate constants (k_1 *and* k_2), q_e and correlation coefficient (R^2) values at 293, 303, and 313 K were listed in Table 4. In accordance with Table 4, all of the correlation coefficients obtained for pseudo-second-order kinetic model were higher than pseudo-first-order kinetic model R^2 values and were close to unity. In the case of pseudo-second order kinetics, the calculated $q_{e,\text{cal}}$ values were very close to the experimental $q_{e,\text{exp}}$ values, while pseudo-first-order model did not give reasonable values. That shows that RY adsorption on SSCAC did not match with the pseudo-first-order model. This result exposed that a chemisorption mechanism most likely controlled the adsorption. Adsorption capacities were increased by raising temperature. This tendency proved that the adsorption occurred endothermically.

3.4. Full Factorial Design of Experiments. Dye removal by an adsorbent in a batch system usually depends on several factors. These are acidity of medium (pH), adsorbent dosage, initial dye concentration, contact time, temperature, and so forth. Only one factor is varied by time and the others are fixed when any factor is optimized; subsequently, the best value obtained by this procedure is fixed and other factors will be varied by the time; thus, using the univariate procedure to optimize all variables is very time consuming. The interactions among all the factors are neglected in univariate procedure, so the best condition could not be achieved [53]. Full factorial design of experiments was performed by practicing with different levels of factors' all probable combinations [54]. The results of the experimental design were analyzed using MINITAB 14 statistical software to evaluate the effects as well as the statistical parameters, the statistical plots (Pareto, normal probability of the standardized effects, main effects, and interaction plots). 2^3 full factorial design having 8 experiments for RY removal was studied, and a matrix was established according to their high and low levels, represented by +1 and −1, respectively. The coded values of variables with the responses (% removal efficiency) were illustrated in Table 5. The interactions between independent factors were determined with analysis of variance (ANOVA) and the main effects of dye adsorption were identified based on the P value with >95% of confidence level.

The following codified equation was used to explain the 2^3 factorial designs of RY removal by SSCAC:

$$Y = X_0 + X_1A + X_2B + X_3C + X_4AB + X_5AC + X_6BC + X_7ABC, \quad (7)$$

where Y is the predicted response (removal efficiency %), X_0 represents the global mean, X_i is the regression coefficient corresponding to the main factor effects and interactions, A is the initial solution pH, B is the adsorbent dose (g/L), and C is the initial dye concentration (mg/L). The main and interaction effects, coefficients of the model, standard deviation of each coefficient, regression coefficients, standard errors, and T and P values were shown in Table 6. All of the main factors (pH, adsorbent dosage, and initial dye concentration) and their interactions (AB) were significant at a 5% of probability level ($P < 0.05$). When the factor effect is negative, removal efficiency decreases as the factor is changed from low to high levels (as seen from pH and initial dye concentration). In contrast, if the effects are positive, removal efficiency increases for high level of the same factor (as seen from adsorbent dosage). Furthermore, the fit models, submitted square correlation coefficient (R^2) of 0.9996, were in good agreement with the statistical model.

Figure 8(a) shows the main effects of the three factors (A, B, and C) on removal efficiency (%). The effect of a factor is the change in response produced by the change in level of factor. This is frequently called a main effect as it refers to the primary factor of interest in the experiment [55]. It was concluded that the larger the vertical line is (see Figure 8(a)), the larger the change in removal efficiency (%) when it is changing from level −1 to level +1. Please note that the statistical significance of a factor is directly related to the length of the vertical line [56]. The ABC effect was insignificant, when it was compared with other effects. Thus the ABC effect was neglected and did not included in the model equation. Then, model equation, related to the level of parameters and removal efficiency, was obtained by substituting the regression coefficients in (7):

$$Y = 21.79 - 10.12A + 10.59B - 6.47C - 5.46AB + 3.47AC - 2.78BC. \quad (8)$$

Equation (8) indicated that two-variable interactions were significant. Proof of large positive (AC) and negative (AB and BC) interactions was quite intense, thus, could not be ignored from the model. Although the main effects gave a clear idea, the interaction between those two parameters would favor a better statement of the process. Figure 8(b)

Table 4: The pseudo-first-order and second-order kinetic parameters for RY dye removal using SSCAC.

Adsorbent dosage (g/50 mL)	T (K)	$q_{e,exp}$ (mg/g)	Pseudo-first-order kinetic model			Pseudo-second-order kinetic model		
			k_1 (min^{-1})	$q_{e,cal}$ (mg/g)	R^2	k_2 (g/(mg∗min))	$q_{e,cal}$ (mg/g)	R^2
0.1	293	12.30	0.02902	4.03	0.863	0.01296	12.80	0.999
	303	12.79	0.02625	6.95	0.734	0.00567	13.81	0.987
	313	16.15	0.02372	5.21	0.894	0.00782	16.92	0.997
0.4	293	8.49	0.01543	3.59	0.759	0.00672	9.23	0.984
	303	9.45	0.01819	4.68	0.801	0.00552	10.37	0.976
	313	10.27	0.04767	8.66	0.826	0.01077	10.96	0.998

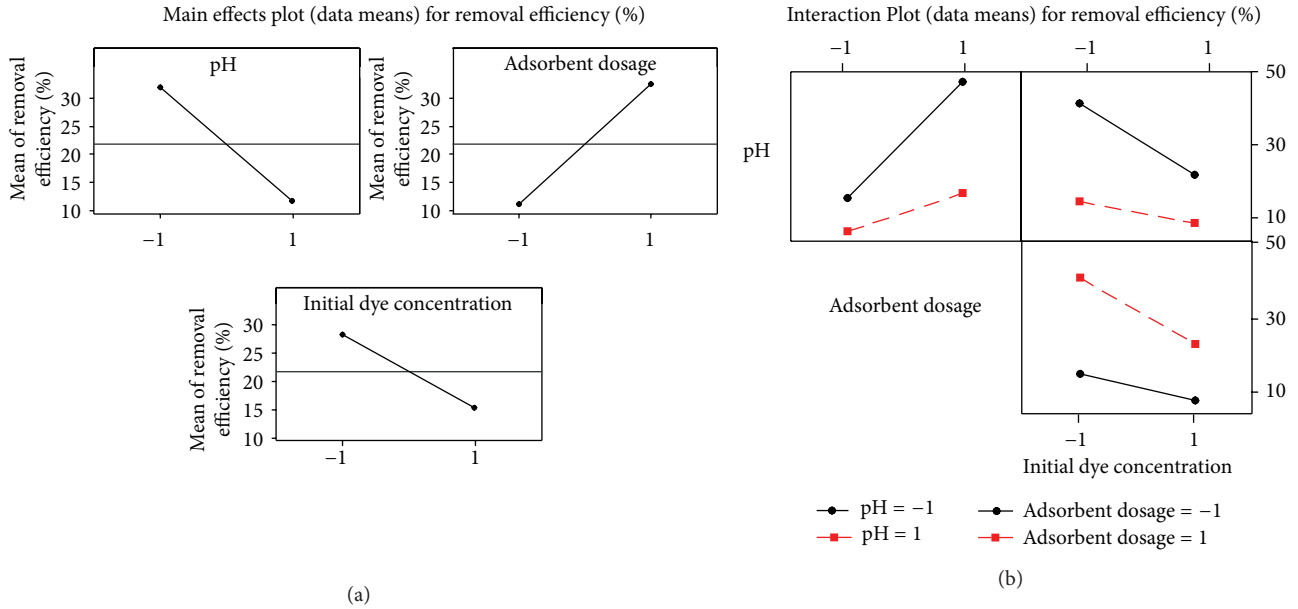

Figure 8: Plots of (a) main effects and (b) interaction effects for the removal efficiency (%).

Table 5: Design matrix for Remazol Yellow.

Runs	pH A	Adsorbent dosage (g/L) B	Dye concentration (mg/L) C	Removal efficiency (%)
1	+1	+1	+1	11.36
2	−1	+1	+1	34.91
3	−1	−1	+1	9.03
4	+1	+1	−1	22.24
5	−1	−1	−1	22.70
6	+1	−1	+1	6.00
7	+1	−1	−1	7.09
8	−1	+1	−1	61.00

obtained from ANOVA illustrated the possible positive and negative two-variable interactions among the variables A, B, and C for removal efficiency (%). It was observed that the effect of pH was more noticeable when the adsorbent dosage was high (see Figure 8(b)), but at lower adsorbent dosage, effect of pH was not so high. On the contrary, pH effect and adsorbent dosage effect were high at lower initial dye concentration.

Figure 9(a) shows the normal probability plot of the standardized effects with $P = 0.05$ to evaluate the significance of each factor and its interactions on removal efficiency (%). Normal probability plot could be separated into two regions, the region with percent above 50% where the factors were indicated positive coefficients (B and AC) and the region with percent below where the factors were indicated negative coefficients (A, C, AB, and AC). All these factors and interactions denoted as a circle were not significant and the effects shown as a square were significant.

Analysis of variance is a statistical method that partitions the total variation into its component parts each of which is associated with a different source of variation [48]. The interaction effects are easily estimated and tested by using the usual ANOVA. The ANOVA results of RY were shown in Table 7. The sum of the squares used to estimate factors affect and Fisher's F ratios (defined as the ratio of mean square effect and the mean square error) and P values (defined as the level of significance leading to the rejection of the null hypothesis) were also represented.

Relative importance of the individual and interaction effects was given by the Pareto chart of the standardized effects in Figure 9(b). In order to identify whether the calculated effects were significantly different from zero, Student's

Table 6: Statistical parameters for 2^3 design.

Term	Effect	Coefficient	Standard error coefficient	T	P
Constant		21.79	0.3287	66.29	0.010
A	−20.74	−10.12	0.3287	−30.78	0.021
B	21.17	10.59	0.3287	32.20	0.020
C	−12.93	−6.47	0.3287	−19.67	0.032
AB	−10.92	−5.46	0.3287	−16.60	0.038
AC	6.95	3.47	0.3287	10.57	0.060
BC	−5.55	−2.78	0.3287	−8.44	0.075
S	0.929845				
R-Sq	99.96%				
R-Sq (adj)	99.75%				

Table 7: Analysis of variance (ANOVA) for removal efficiency (%).

Source	DF	Sum of squares (SS)	Mean square (MS)	F	P value
A	1	819.11	819.11	947.38	0.021
B	1	896.55	896.55	1036.94	0.020
C	1	334.50	334.50	386.88	0.032
$A * B$	1	238.38	238.38	275.71	0.038
$A * C$	1	96.54	96.54	111.65	0.060
$B * C$	1	61.66	61.66	71.32	0.075
Error	1	0.86	0.86		
Total	7	2447.61			
Main effects	3	2050.16	683.387	790.40	0.026
2-way interactions	3	396.58	132.193	152.89	0.059
Residual error	1	0.86	0.865		
Total	7	2447.61			

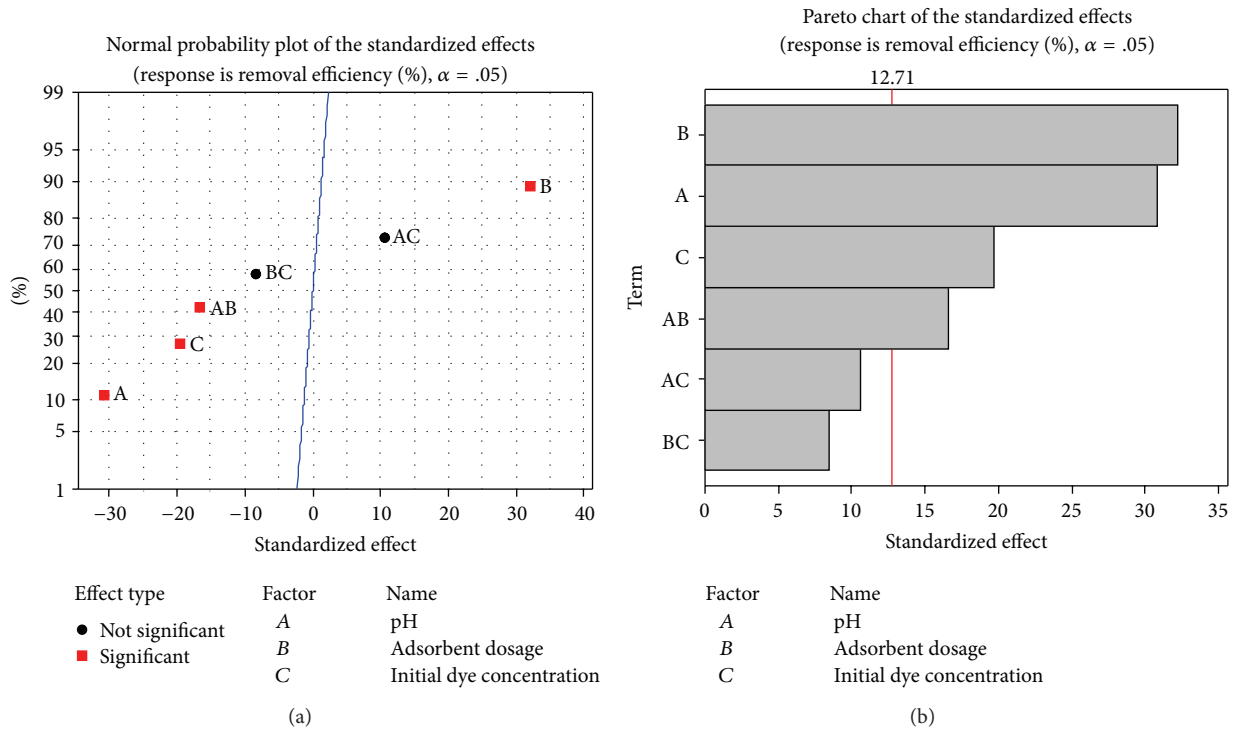

Figure 9: (a) Normal probability plot of the standardized effects at $P = 0.05$, (b) Pareto chart of standardized effects on the removal efficiency (%) for RY.

t-test was performed and horizontal columns in Pareto chart showed these values for each effect. For a 95% confidence level and seven degrees of freedom t value was equal to 12.71. The minimum statistically significant effect magnitude for 95% confidence level is represented by the vertical line in the chart. Four values higher than 12.71 ($P = 0.05$) were located at right of the dash line and were significant.

It can be concluded that the adsorbent dosage was the strongest effect of the overall adsorption procedure of SSCAC. The $X2$ coefficient was the largest negative coefficient for model equation (8). The positive value of its coefficient meant that RY removal by SSCAC was preferred at adsorbent dosage of 8 g/L. An increase of adsorbent dosage caused an uptrend in the percentage removal of RY dye, since rising adsorbent dosage provided a suitable surface area for adsorption. The second important factor to the overall optimization of the batch adsorption process was pH. The increase in the pH involved a striking decrease of RY uptake by SSCAC. The third important factor was the initial dye concentration of dye. Surface area and active sites of SSCAC may be saturated at higher concentrations; thus, removal efficiency (%) decreased with raising the initial dye concentration. The interaction of two factors AB was the fourth significant factor. The coefficient of this interaction had the negative value; thus, a decrease in pH of the solution with a deduction of the adsorbent dosage caused an increase in removal efficiency (%). This antagonistic effect would not be distinguished in the univariate optimization of the dye removal process.

4. Conclusions

Green carbon produced by chemical activation of sunflower seed cake with an activation agent 50% NH_4Cl was capable of removing reactive Remazol Yellow dye molecules from aqueous solutions. The adsorption was favored at acidic medium with pH value 2 and adsorption efficiency (%) was also found to increase with the increase in adsorbent dosage, contact time, temperature, and addition of electrolyte. The kinetic study showed that dye-activated carbon adsorption systems followed by pseudo-second-order model with high correlation coefficients and the process was endothermic. The equilibrium data was in good agreement with the Langmuir model and dimensionless separation factors (R_L values) within the range of zero to one showed that the adsorption was favorable. Additionally, the influence of pH (2–8), adsorbent dosage (2–8 g/L), and initial dye concentration (100–250 mg/L) on removal efficiency (%) was designed by using 2^3 full factorial design. It was examined by using analysis of variance (ANOVA), t-test, and F-test. According to Pareto Chart, normal probability plot, main effects, and interaction plots in variance analysis, the most significant factors on removal efficiency (%) were found to be adsorbent dosage (B), pH (A), initial dye concentration (C), and the interaction between pH and adsorbent dosage (AB), respectively. Conversely, the other interactions were not effective on RY adsorption. Due to the obtained results, green carbon which is produced from chemical activation of sunflower seed cake could be employed as an effective and low-cost adsorbent. Therefore, this successful adsorbent could be considered as an alternate to commercial activated carbons for the removal of reactive remazol yellow dye from aqueous solutions.

References

[1] E. N. El Qada, S. J. Allen, and G. M. Walker, "Adsorption of basic dyes from aqueous solution onto activated carbons," *Chemical Engineering Journal*, vol. 135, no. 3, pp. 174–184, 2008.

[2] T. Shen, *Industrial Pollution Prevention*, Spring, Berlin, Germany, 1995.

[3] P. Cooper, "Removing colour from dyehouse wastewaters—a critical review of technology available," *Journal of the Society of Dyers and Colourists*, vol. 109, no. 3, pp. 97–100, 1993.

[4] S. B. Jadhav, S. S. Phugare, P. S. Patil, and J. P. Jadhav, "Biochemical degradation pathway of textile dye Remazol red and subsequent toxicological evaluation by cytotoxicity, genotoxicity and oxidative stress studies," *International Biodeterioration and Biodegradation*, vol. 65, no. 6, pp. 733–743, 2011.

[5] V. K. Gupta, B. Gupta, A. Rastogi, S. Agarwal, and A. Nayak, "A comparative investigation on adsorption performances of mesoporous activated carbon prepared from waste rubber tire and activated carbon for a hazardous azo dye—Acid Blue 113," *Journal of Hazardous Materials*, vol. 186, no. 1, pp. 891–901, 2011.

[6] M. F. Elkady, A. M. Ibrahim, and M. M. A. El-Latif, "Assessment of the adsorption kinetics, equilibrium and thermodynamic for the potential removal of reactive red dye using eggshell biocomposite beads," *Desalination*, vol. 278, no. 1–3, pp. 412–423, 2011.

[7] G. S. Gupta, S. P. Shukla, G. Prasad, and V. N. Singh, "China clay as an adsorbent for dye house wastewaters," *Environmental Technology*, vol. 13, no. 10, pp. 925–936, 1992.

[8] J. Sokolowska-Gajda, H. S. Freeman, and A. Reife, "Synthetic dyes based on environmental considerations. Part 2: iron complexed formazan dyes," *Dyes and Pigments*, vol. 30, no. 1, pp. 1–20, 1996.

[9] O. Tünay, I. Kabdaşli, D. Orhon, and G. Cansever, "Use and minimization of water in leather tanning processes," *Water Science and Technology*, vol. 40, no. 1, pp. 237–244, 1999.

[10] K. Ivanov, E. Gruber, W. Schempp, and D. Kirov, "Possibilities of using zeolite as filler and carrier for dyestuffs in paper," *Das Papier*, vol. 4, no. 7-8, pp. 450–456, 1996.

[11] A. Slampova, D. Smela, A. Vondrackova, I. Jancarova, and V. Kuban, "Determination of synthetic colorants in foodstuffs," *Chemicke Listy*, vol. 95, pp. 163–168, 2001.

[12] S. M. F. Cook and D. R. Linden, "Use of rhodamine WT to facilitate dilution and analysis of atrazine samples in short-term transport studies," *Journal of Environmental Quality*, vol. 26, no. 5, pp. 1438–1440, 1997.

[13] R. W. Wagner and J. S. Lindsey, "Boron-dipyrromethene dyes for incorporation in synthetic multi-pigment light-harvesting arrays," *Pure and Applied Chemistry*, vol. 68, no. 7, pp. 1373–1380, 1996.

[14] D. Wróbel, A. Boguta, and R. M. Ion, "Mixtures of synthetic organic dyes in a photoelectrochemical cell," *Journal of Photochemistry and Photobiology A*, vol. 138, no. 1, pp. 7–22, 2001.

[15] C. Scarpi, F. Ninci, M. Centini, and C. A. Cecilia Anselmi, "High-performance liquid chromatography determination of direct and temporary dyes in natural hair colourings," *Journal of Chromatography A*, vol. 796, no. 2, pp. 319–325, 1998.

[16] A. Srinivasan and T. Viraraghavan, "Decolorization of dye wastewaters by biosorbents: a review," *Journal of Environmental Management*, vol. 91, no. 10, pp. 1915–1929, 2010.

[17] P. Kaushik and A. Malik, "Fungal dye decolourization: recent advances and future potential," *Environment International*, vol. 35, no. 1, pp. 127–141, 2009.

[18] M. A. Ahmad and N. K. Rahman, "Equilibrium, kinetics and thermodynamic of Remazol Brilliant Orange 3R dye adsorption on coffee husk-based activated carbon," *Chemical Engineering Journal*, vol. 170, no. 1, pp. 154–161, 2011.

[19] M. A. Ahmad and R. Alrozi, "Optimization of rambutan peel based activated carbon preparation conditions for Remazol Brilliant Blue R removal," *Chemical Engineering Journal*, vol. 168, no. 1, pp. 280–285, 2011.

[20] K. Santhy and P. Selvapathy, "Removal of reactive dyes from wastewater by adsorption on coir pith activated carbon," *Bioresource Technology*, vol. 97, no. 11, pp. 1329–1336, 2006.

[21] I. M. Banat, P. Nigam, D. Singh, and R. Marchant, "Microbial decolorization of textile-dye-containing effluents: a review," *Bioresource Technology*, vol. 58, pp. 217–227, 1996.

[22] V. K. Konaganti, R. Kota, S. Patil, and G. Madras, "Adsorption of anionic dyes on chitosan grafted poly(alkyl methacrylate)s," *Chemical Engineering Journal*, vol. 158, no. 3, pp. 393–401, 2010.

[23] A. Gürses, Ç. Doğar, S. Karaca, M. Açikyildiz, and R. Bayrak, "Production of granular activated carbon from waste *Rosa canina* sp. seeds and its adsorption characteristics for dye," *Journal of Hazardous Materials*, vol. 131, no. 1–3, pp. 254–259, 2006.

[24] D. D. Asouhidou, K. S. Triantafyllidis, N. K. Lazaridis, and K. A. Matis, "Adsorption of Remazol Red 3BS from aqueous solutions using APTES- and cyclodextrin-modified HMS-type mesoporous silicas," *Colloids and Surfaces A*, vol. 346, no. 1–3, pp. 83–90, 2009.

[25] G. Crini, "Non-conventional low-cost adsorbents for dye removal: a review," *Bioresource Technology*, vol. 97, no. 9, pp. 1061–1085, 2006.

[26] K. R. Ramakrishna and T. Viraraghavan, "Dye removal using low cost adsorbents," *Water Science and Technology*, vol. 36, no. 2-3, pp. 189–196, 1997.

[27] V. K. Gupta and S. Suhas, "Application of low-cost adsorbents for dye removal—a review," *Journal of Environmental Management*, vol. 90, no. 8, pp. 2313–2342, 2009.

[28] A. Mittal, D. Kaur, and J. Mittal, "Applicability of waste materials-bottom ash and deoiled soya-as adsorbents for the removal and recovery of a hazardous dye, brilliant green," *Journal of Colloid and Interface Science*, vol. 326, no. 1, pp. 8–17, 2008.

[29] Z. Aksu and I. A. Isoglu, "Use of agricultural waste sugar beet pulp for the removal of Gemazol turquoise blue-G reactive dye from aqueous solution," *Journal of Hazardous Materials*, vol. 137, no. 1, pp. 418–430, 2006.

[30] N. K. Amin, "Removal of reactive dye from aqueous solutions by adsorption onto activated carbons prepared from sugarcane bagasse pith," *Desalination*, vol. 223, no. 1–3, pp. 152–161, 2008.

[31] S. Senthilkumaar, P. Kalaamani, K. Porkodi, P. R. Varadarajan, and C. V. Subburaam, "Adsorption of dissolved Reactive red dye from aqueous phase onto activated carbon prepared from agricultural waste," *Bioresource Technology*, vol. 97, no. 14, pp. 1618–1625, 2006.

[32] V. K. Gupta, A. Mittal, L. Kurup, and J. Mittal, "Adsorption of a hazardous dye, erythrosine, over hen feathers," *Journal of Colloid and Interface Science*, vol. 304, no. 1, pp. 52–57, 2006.

[33] V. K. Gupta, A. Mittal, A. Malviya, and J. Mittal, "Adsorption of carmoisine A from wastewater using waste materials—Bottom ash and deoiled soya," *Journal of Colloid and Interface Science*, vol. 335, no. 1, pp. 24–33, 2009.

[34] A. Mittal, L. Kurup, and V. K. Gupta, "Use of waste materials—Bottom Ash and De-Oiled Soya, as potential adsorbents for the removal of Amaranth from aqueous solutions," *Journal of Hazardous Materials*, vol. 117, no. 2-3, pp. 171–178, 2005.

[35] V. K. Gupta, R. Jain, and S. Varshney, "Removal of Reactofix golden yellow 3 RFN from aqueous solution using wheat husk—an agricultural waste," *Journal of Hazardous Materials*, vol. 142, no. 1-2, pp. 443–448, 2007.

[36] K. Y. Foo and B. H. Hameed, "Preparation and characterization of activated carbon from sunflower seed oil residue via microwave assisted K_2CO_3 activation," *Bioresource Technology*, vol. 102, no. 20, pp. 9794–9799, 2011.

[37] National Sunflower Association, Sunflower Statistics, 2012, http://www.sunflowernsa.com/stats/world-supply.

[38] B. H. Hameed, "Equilibrium and kinetic studies of methyl violet sorption by agricultural waste," *Journal of Hazardous Materials*, vol. 154, no. 1–3, pp. 204–212, 2008.

[39] M. Cantamutto and M. Poverene, "Genetically modified sunflower release: opportunities and risks," *Field Crops Research*, vol. 101, no. 2, pp. 133–144, 2007.

[40] Z.-Y. Zhong, Q. Yang, X.-M. Li, K. Luo, Y. Liu, and G.-M. Zeng, "Preparation of peanut hull-based activated carbon by microwave-induced phosphoric acid activation and its application in Remazol Brilliant Blue R adsorption," *Industrial Crops and Products*, vol. 37, no. 1, pp. 178–185, 2012.

[41] P. Sathishkumar, M. Arulkumar, and T. Palvannan, "Utilization of agro-industrial waste Jatropha curcas pods as an activated carbon for the adsorption of reactive dye Remazol Brilliant Blue R (RBBR)," *Journal of Cleaner Production*, vol. 22, no. 1, pp. 67–75, 2012.

[42] M. Jain, V. K. Garg, and K. Kadirvelu, "Equilibrium and kinetic studies for sequestration of Cr(VI) from simulated wastewater using sunflower waste biomass," *Journal of Hazardous Materials*, vol. 171, no. 1–3, pp. 328–334, 2009.

[43] A. P. Vieira, S. A. A. Santana, C. W. B. Bezerra et al., "Kinetics and thermodynamics of textile dye adsorption from aqueous solutions using babassu coconut mesocarp," *Journal of Hazardous Materials*, vol. 166, no. 2-3, pp. 1272–1278, 2009.

[44] A. Y. Dursun and O. Tepe, "Removal of Chemazol Reactive Red 195 from aqueous solution by dehydrated beet pulp carbon," *Journal of Hazardous Materials*, vol. 194, pp. 303–311, 2011.

[45] K. E. Lee, N. Morad, T. T. Teng, and B. T. Poh, "Factorial experimental design for reactive dye flocculation using inorganic-organic composite polymer," *APCBEE Procedia*, vol. 1, pp. 59–65, 2012.

[46] G. Annadurai, R.-S. Juang, and D.-J. Lee, "Factorial design analysis for adsorption of dye on activated carbon beads incorporated with calcium alginate," *Advances in Environmental Research*, vol. 6, no. 2, pp. 191–198, 2002.

[47] V. Ponnusami, V. Krithika, R. Madhuram, and S. N. Srivastava, "Biosorption of reactive dye using acid-treated rice husk: factorial design analysis," *Journal of Hazardous Materials*, vol. 142, no. 1-2, pp. 397–403, 2007.

[48] Y. Safa and H. N. Bhatti, "Adsorptive removal of direct textile dyes by low cost agricultural waste: application of factorial design analysis," *Chemical Engineering Journal*, vol. 167, no. 1, pp. 35–41, 2011.

[49] N. F. Cardoso, R. B. Pinto, E. C. Lima et al., "Removal of remazol black B textile dye from aqueous solution by adsorption," *Desalination*, vol. 269, no. 1–3, pp. 92–103, 2011.

[50] Z. Mbolekwa and C. Buckley, "Dye removal with activated carbon for the reuse of salt, water and energy," Industrial Wastewater Treatment, WISA, 2006.

[51] S. M. A. Guelli Ulson de Souza, L. C. Peruzzo, and A. A. Ulson de Souza, "Numerical study of the adsorption of dyes from textile effluents," *Applied Mathematical Modelling*, vol. 32, no. 9, pp. 1711–1718, 2008.

[52] F. R. Furlan, L. G. de Melo da Silva, A. F. Morgado, A. A. U. de Souza, and S. M. A. Guelli Ulson de Souza, "Removal of reactive dyes from aqueous solutions using combined coagulation/flocculation and adsorption on activated carbon," *Resources, Conservation and Recycling*, vol. 54, no. 5, pp. 283–290, 2010.

[53] E. C. Lima, B. Royer, J. C. P. Vaghetti et al., "Adsorption of Cu(II) on Araucaria angustifolia wastes: determination of the optimal conditions by statistic design of experiments," *Journal of Hazardous Materials*, vol. 140, no. 1-2, pp. 211–220, 2007.

[54] Y. Safa and H. N. Bhatti, "Biosorption of direct red-31 and direct orange-26 dyes by rice husk: application of factorial design analysis," *Chemical Engineering Research and Design*, vol. 89, no. 12, pp. 2566–2574, 2011.

[55] A. Rathinam, J. R. Rao, and B. U. Nair, "Adsorption of phenol onto activated carbon from seaweed: determination of the optimal experimental parameters using factorial design," *Journal of the Taiwan Institute of Chemical Engineers*, vol. 42, no. 6, pp. 952–956, 2011.

[56] D. Bingol, N. Tekin, and M. Alkan, "Brilliant Yellow dye adsorption onto sepiolite using a full factorial design," *Applied Clay Science*, vol. 50, no. 3, pp. 315–321, 2010.